Extraordinary Transmission of Metal Films with Arrays of Subwavelength Holes

James V. Coe, Joseph M. Heer, Shannon Teeters-Kennedy, Hong Tian, and Kenneth R. Rodriguez

Department of Chemistry, The Ohio State University, Columbus, Ohio 43210-1173; email: coe.1@osu.edu

Annu. Rev. Phys. Chem. 2008. 59:179–202

First published online as a Review in Advance on November 7, 2007

The *Annual Review of Physical Chemistry* is online at http://physchem.annualreviews.org

This article's doi: 10.1146/annurev.physchem.59.032607.093703

0066-426X/08/0505-0179$20.00

Key Words

surface plasmons, plasmonics, photonic metal mesh, surface-enhanced infrared spectroscopy, Raman spectroscopy

Abstract

Metal films with patterns of subwavelength holes (grids or meshes) have interesting optical properties including the extraordinary transmission effect. These optically thick metal films transmit more radiation than that incident on the holes owing to the excitation of surface plasmons (SPs). Meshes present a new and simple way to excite SPs at perpendicular incidence (i.e., without the need to vary the angle of the incident beam). This represents a new opportunity to integrate SPs with experiments and devices—a new instrument in the toolbox of SP techniques that may broaden the range of SP applications. This review discusses the discovery, basic optical physics, the role of SPs, and applications of the extraordinary transmission of subwavelength hole arrays.

INTRODUCTION

SP: surface plasmon

A smooth metal film, with a thickness that would transmit little incident radiation, can be made to transmit radiation efficiently by perforating the metal film with an array of subwavelength holes (1–4) (see **Figure 1**). Investigators have studied metallic mesh arrays (often described as inductive grids) in the far-infrared region since the 1960s (5–7). Recent interest has been piqued by the role of surface plasmons (SPs) in the visible (1, 8, 9), more recently the mid-infrared (2, 10, 11), and the terahertz (12) region. Noting that the extraordinary transmission of subwavelength hole arrays is characterized as transmittance divided by the fractional open area of holes, we can see that the mesh in **Figure 1** demonstrates an enhancement factor of 3.4 on its primary transmission resonance. A large fraction of incident radiation initially hits metal but still is transmitted with optical fidelity. The explanation of extraordinary transmission involves a role for SPs (1, 9, 13, 14), both propagating and localized. Metal films with subwavelength hole arrays are now considered new plasmonic metamaterials (15). There is great interest in SPs (8, 16–18) because they exhibit the following: high electric fields at the surface of the metal (19–21) (good for surface-enhanced Raman spectroscopy), reduced wavelengths relative to the incident radiation [good for subwavelength imaging (22), near-field scanning optical microscopy (23)], increased transmission [good for superlensing (24, 25)], two-dimensionality (10)

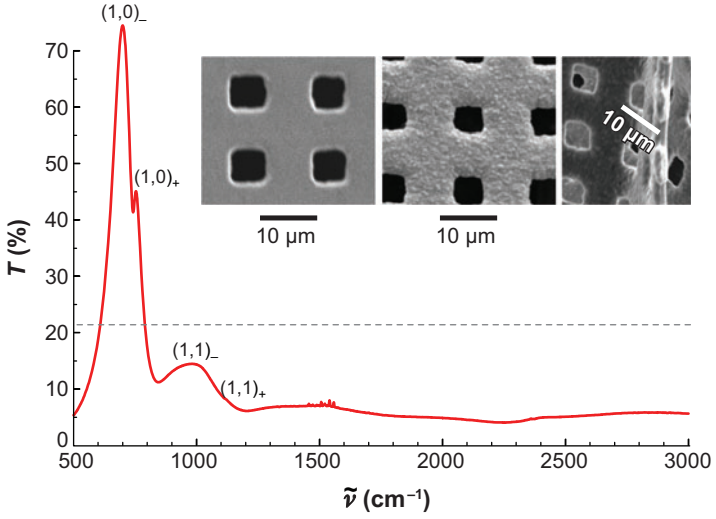

Figure 1

Zero-order Fourier transform infrared spectroscopy (FTIR) transmission spectrum of an Ni mesh (from Precision Eforming, Coutland, New York) with square holes on a square lattice (lattice parameter $L = 12.7$ μm, hole width $a = 6.0$ μm, thickness $b = 3$ μm). (*Inset*) Scanning electron microscope images. The gray dotted line represents the percentage of the holes' open area. A 74% transmission on the primary resonance (3.4 times the open area) suggests that much radiation hits the optically thick metal and is transported along the metal surface until it emerges through the holes without being scattered from the FTIR spectrometer's beam (i.e., it exhibits Ebbesen's extraordinary transmission effect).

(good for probing subwavelength nanospaces), the potential for bridging photonics and electronics (plasmonics) (26), sensitivity as sensors (17) for bioanalytical assays [SP-attenuated total reflection (SP-ATR)], and more efficient fluorescence collection (27, 28) using SP coupled emission or enhanced absorption spectroscopy in the infrared (29) and visible (30). SPs can change the balance of fundamental relationships. For instance, if Young's classic two-slit experiment is done with metal slits, the intensity of the far-field pattern can be reduced or enhanced, depending on SP propagation between the slits (31). SPs offer a new set of tools for accomplishing experiments in small spaces, with high electric fields and/or long path lengths for absorption.

SP-ATR: surface plasmon attenuated total reflection

LSP: localized surface plasmon

WHAT ARE PROPAGATING SURFACE PLASMONS AND HOW ARE THEY CHARACTERIZED?

SPs are essentially light trapped at a metal's surface by its interaction with the metal's conducting electrons, which act like a plasma. Localized SPs (LSPs) (16, 17) are excited by light on isolated particles much smaller than the wavelength, such as metal nanoparticles (32). The incident light excites an oscillation of the particle's cloud of conducting electrons that is localized on the particle. Such excitations can be transferred to similar, adjacent structures if they are sufficiently close (18, 33). Periodic arrays of coupled particles enable excitations to propagate along the arrays like ripples on a pond.

We can understand the underlying physics of propagating SPs in terms of an SP dispersion curve in momentum space (34, 35) (**Figure 2**). The SP curve in

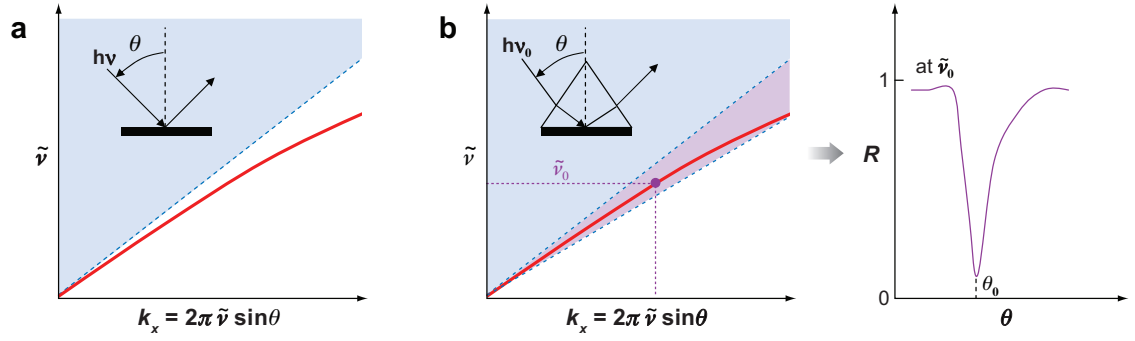

Figure 2

(*a*) Dispersion diagram for a smooth air/metal interface. The light line is represented by a blue dotted line, and the surface plasmon (SP) curve is represented by a solid red line. These plots give the reciprocal wavelength ($\tilde{\nu}$) versus the real component of the momentum wave vector parallel to the surface ($k_x = 2\pi\tilde{\nu}\sin\theta$, where θ is the angle of the incident beam relative to the surface normal). The blue shading indicates the region accessible by the angular variation of an incident beam (from the z axis of the surface normal toward the x axis of the surface). The SP curve lies outside the light line and is not accessible. (*b*) The use of a prism with a thin metal coating additionally makes the purple shaded region accessible, which now overlaps with the SP curve. At a specific wave number of light ($\tilde{\nu}_0$), one can access the SP at a specific value of the momentum wave vector. This is often detected by scanning the reflectance as a function of angle (θ) (*right panel*) producing a dip in the reflection on resonance versus θ.

Figure 2 lies outside the accessible region bounded by the light line [$\tilde{\nu} = k_x/(2\pi)$], so SPs cannot be excited on a smooth air/metal interface by incident light. At any specific wavelength, SPs have momentum greater than incident photons at the air/metal interface, so some feature of the interface must add momentum to the photons to excite SPs. Typically investigators use prisms, gratings, or surface roughness to couple light to SPs (34). There was a sudden increase in propagating SP research in the late 1960s when Otto (36), followed closely by Kretschmann & Raether (37), demonstrated SP-ATR (see **Figure 2*b***). In these experiments, they reflected a fixed-frequency laser from a prism with a nanoscale thin metal coating. The index of refraction (n) of the prism shifts the light line [by $\tilde{\nu} = k_x/(2\pi n)$], allowing the green region to be additionally accessed (**Figure 2*b***). At a fixed reciprocal wavelength ($\tilde{\nu}_0$), there is a fixed value of k_x (and therefore a fixed value of the angle, θ_0) at which SPs can be excited. Typically experiments proceed by monitoring a dip in reflectance (R), when SPs are excited along the air/metal interface, as a function of θ of a fixed wavelength source (see **Figure 2*b***). Once excited, the SPs propagate along the smooth and flat metal surface (at a large fraction of the speed of light in vacuum) until they dissipate, scatter, or radiate, perhaps at macroscopic distances from their origin. The normal reflectivity of the metal surface is greatly reduced on resonance.

PROPAGATING SURFACE PLASMONS ON GRIDS

The excitation of SPs on grids (bigratings or two-dimensional gratings) is more complicated. It involves SP excitation by subwavelength structures in the periodic lattice, SP propagation along the metal surface with reflection at holes (a band structure), propagation on both sides of the periodic lattice by tunneling through the holes (coupling of the front and back surfaces), and finally SP conversion back into photons by radiation damping at the hole structures—probably involving the LSP properties of the holes (38, 39). Much of this occurs without scattering the light or damaging the modulation optics of ordinary spectrometers. Bigratings have some resonant features that are similar to those of SP-ATR and others that are different. If a metallic array of subwavelength holes is active with propagating SPs, then an SP dispersion curve should exist that characterizes its behavior. We determine these curves in the next section below. However, some preliminary discussion is useful to understand the pending results.

Some of the earliest work on SPs (40–44) pertains to one-dimensional gratings although SPs were not identified as such until the 1960s (45, 43). If a metal film is corrugated with a one-dimensional periodic pattern of slits, then the surface can transfer momentum in units of $2\pi/L$, where L is the slit-to-slit spacing. Schroter & Heitmann (46) have studied the SP behavior of this system. The SP dispersion curve manifests itself with a Brillouin periodicity, resulting in access within the light line as shown in **Figure 3*a*** for the defined geometry. The actual states avoid the crossings producing band gaps (45), and the features are only excited with p-polarized light.

The meshes discussed in this review are bigratings with holes oriented in both the x and y directions, so they gain momentum in units of $2\pi/L$ in either the x or y directions [i.e., as the magnitude of $(2\pi/L)\,i\hat{\mathbf{x}} + (2\pi/L)\,j\hat{\mathbf{y}}$, where i and j are

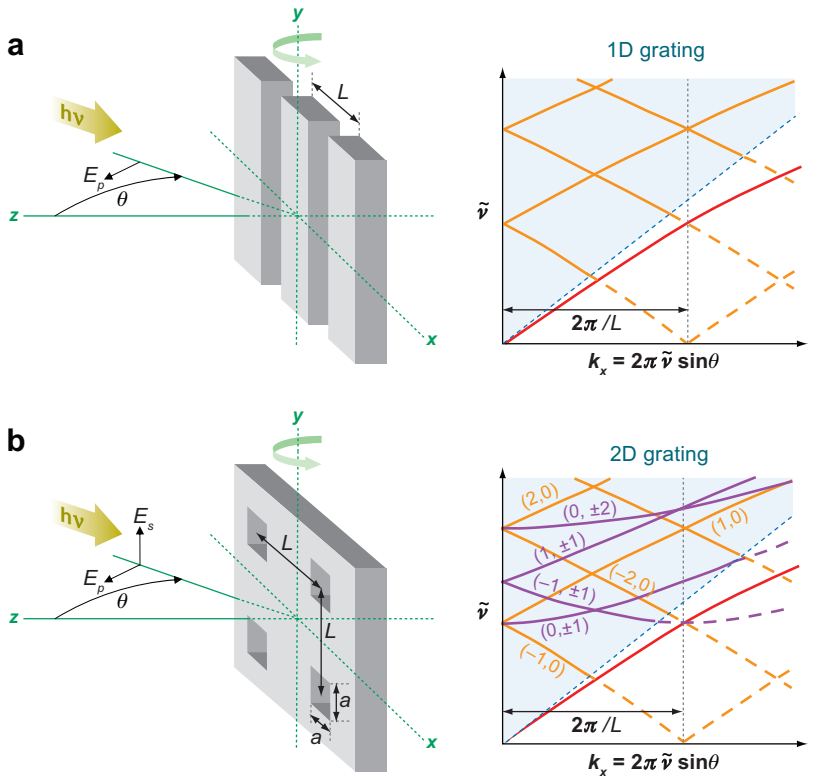

Figure 3

(*a*) Dispersion curve (*right panel*) of a one-dimensional grating of slits for the defined geometry (*left panel*). This gives rise to *p*-polarized dispersion curves. The red surface plasmon (SP) dispersion curve is replicated in units of $2\pi/L$ (and reflected at $k_x = 0$) owing to the periodicity of the structure. This produces SP access within the light line (*solid orange curves*) and typical *p*-polarized dispersion trends. The solid orange lines give rise to leaky modes because they interact with light. (*b*) Dispersion curve (*right panel*) of a two-dimensional grating of a square lattice of holes for the defined geometry (*left panel*). *L* is the lattice parameter (hole center to hole center spacing), *a* is the square hole width, and *h* is the thickness of the film. Holes are aligned along the *x* and *y* axes, and light is incident along the *z* axis when $\theta = 0$. The transmission resonances at low momentum wave vectors are labeled by (i, j). The arrangement gives rise to components of the surface momentum in both the *x* and *y* directions. The contributions of the *y* components of surface momentum to the magnitude of momentum give rise to the purple curves, in addition to the orange curves, which are *p*-polarized and similar to the one-dimensional case. The purple curves have at least some *s*-polarized character.

steps along the reciprocal lattice]. The indices (i, j) both label the resonances and correspond to the diffraction spots that are no longer transmitted at the wavelengths of the transmission resonances. A coordinate system and geometrical parameters are defined for a mesh with a square lattice of square holes in **Figure 3*b***. With bigratings, momentum gained from the *y* component projects onto the k_x picture of **Figure 3*a***, giving rise to additional curves with some *s*-polarized character in **Figure 3*b*** (47).

Bigratings differ in many features compared with their one-dimensional analogs, including a higher density of resonances, some resonances with different dispersion, and some resonances with partial or full *s*-polarized character. Grating coupling and momentum matching give the position of the propagating SP resonances (away from the band gaps) as

$$\tilde{\nu}_{i,j}(k_x) = \frac{1}{2\pi n'_{eff}}\sqrt{\left(k_x + \frac{2\pi i}{L}\right)^2 + \left(\frac{2\pi j}{L}\right)^2}, \quad (1)$$

for the geometry given in **Figure 3*b*** (called the ΓX orientation), where n'_{eff} is the real part of the effective index of refraction of the mesh interface, which can vary with wavelength and coating dielectric. (This expression describes the SP curve shown in **Figure 3*b*** when $i, j = 0, 0$, which lies outside the light line.) Ulrich described this mode as nonleaky and demonstrated how to access it on mesh using a pair of prism couplers (4; see figure 6 therein). The (i, j) resonances on square lattice bigratings with at least one nonzero value of either i or j can be inside the light line (i.e., can be excited by incident light) and have been described as leaky modes (4). With $k_x = 0$, this expression describes the position of resonances at perpendicular incidence. With multiple resonances, one can observe useful transmission over extended frequency ranges. For instance, the meshes with 12.7-μm lattice parameters used by the Coe group (see **Figure 1**) cover most of the range of fundamental molecular vibrations, which is useful for infrared spectroscopy. Ulrich seems to have observed the first SPs on bigratings (not one-dimensional gratings) in the far infrared at approximately 80 cm^{-1} (4; see figure 2 therein). He described metal mesh as a "periodic, open wave guide structure" with surface waves that "can be understood as Zenneck waves propagating on both sides of the mesh, being coupled and perturbed by the periodic perforation." He also described front-back coupling and measured the dispersion of the resonances. Derrick et al. also may have observed propagating SPs (although not identified as such) on gold grids in the visible (6; see figure 4 therein), but the field took off with Ebbesen and coworkers' (1) observations on nanohole arrays in metal films indicating a role for SPs. (This paper has been cited 1003 times at the writing of this review.)

EVIDENCE FOR THE ROLE OF PROPAGATING SURFACE PLASMONS ON GRIDS

The dispersion behavior (position of resonances versus k_x) is one of the most important observations supporting a role for propagating SPs. Ebbesen and coworkers (1, 9, 14, 48, 49) have measured the dispersion of grid transmission resonances (usually circular holes on square lattices). **Figure 4** presents the determination of the SP dispersion curve using Ebbesen's data for the position of the (−1,0) resonance of two freestanding silver films (49; see figure 3 therein). To cast this data in the same context as **Figures 2** and **3**, we reflect it at the $k_x = 0$ line and translate it by $2\pi/L$ (grating coupling) to reach the region near the light line. The open-diamond form is similar to that of zero-order propagating SPs on a smooth air/metal interface, but it is pushed to a lower slope $[1/(2\pi n'_{eff})]$ in momentum space by n'_{eff} (greater than the smooth

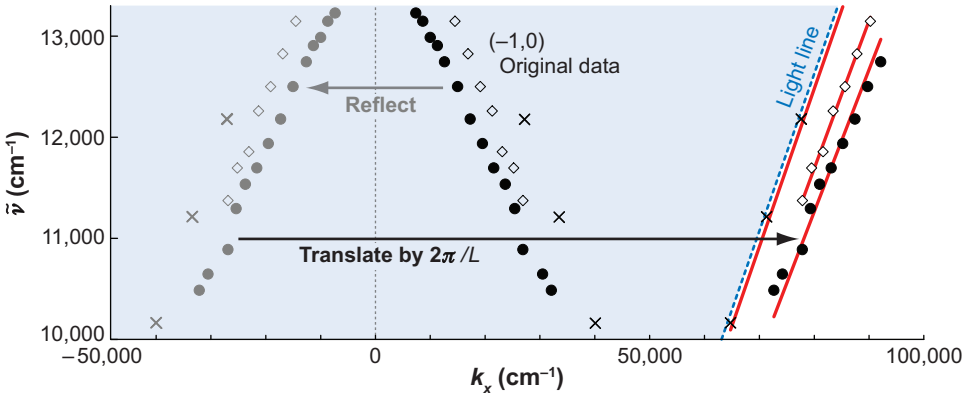

Figure 4

Original peak positions of the (–1,0) resonance from the Ebbesen group's grids reflected and translated by $2\pi/L$ (grating coupling) to access the region of the light line. The data were fit away from the band gap to surface plasmon (SP) dispersion curves of the form $\tilde{\nu}(k_x) = k_x/(2\pi n'_{eff})$ giving values of n'_{eff}. The x symbols represent the zero-order expectation for SPs on a smooth air/metal interface, and $n'_{eff} = 1.020$, arising from (34, 50) $n'_{eff} = \mathrm{Re}\{\sqrt{(\varepsilon_m \varepsilon_s)/(\varepsilon_m + \varepsilon_s)}\}$, where ε_m and ε_s are the complex dielectrics of the metal and substrate medium, respectively. The open-diamond symbols correspond to a thicker mesh ($L = 600$ nm, circular holes of 300-nm diameter, and $h = 570$ nm) giving a fit (*red line*) to $n'_{eff} = 1.089$. The filled-circle symbols correspond to a thinner mesh (same dimensions as for the thicker mesh, except $h = 300$ nm). The thinner mesh is pushed farther from the light line owing to the stronger coupling of SPs on the front and back sides through the holes. Shifts from the zero-order, smooth metal expectation of this size are known for coupled smooth metal interfaces spaced by approximately one wavelength of the incident light.

metal expectation by 0.069). A clue is offered about the nature of the shift by the data set for a thinner mesh ($h = 300$ nm). The fit to this data set gives $n'_{eff} = 1.131$, which pushes the slope lower than the smooth air/metal expectation by an excess of 0.111 of refraction index. The thinner film corresponds to stronger coupling between SPs on the front and back sides, which pushes the SP dispersion curve to higher momentum.

Researchers have obtained similar results working in the mid-infrared region (11) using freestanding Ni mesh (square holes on a square lattice, $L = 12.7$ μm, $a = 5.2$ μm, and $h = 3.0$ μm) (**Figure 5**). The measured transmission resonance peak centers (**Figure 5*a***) project, by bigrating momentum-matching equations (47), onto two SP dispersion curves (**Figure 5*b***): One lies directly on the light line ($n'_{eff} = 1.000$, which is also the zero-order expectation for smooth air/metal interfaces in the infrared), and the other is well modeled by $n'_{eff} = 1.061$, which again corresponds to a lower slope in momentum space by an excess of 0.061 units of refractive index. Although the Ebbesen group noted some features of strong front-back coupling, it has not been widely appreciated that the grid shifts are in line with the first- (and second-) order shifts seen on coupled smooth metal interfaces in the SP-ATR experiments (51–53). Teeters-Kennedy et al. summarized such results (10; see equation 7 therein), showing grid shifts similar to coupled smooth metal interfaces spaced by

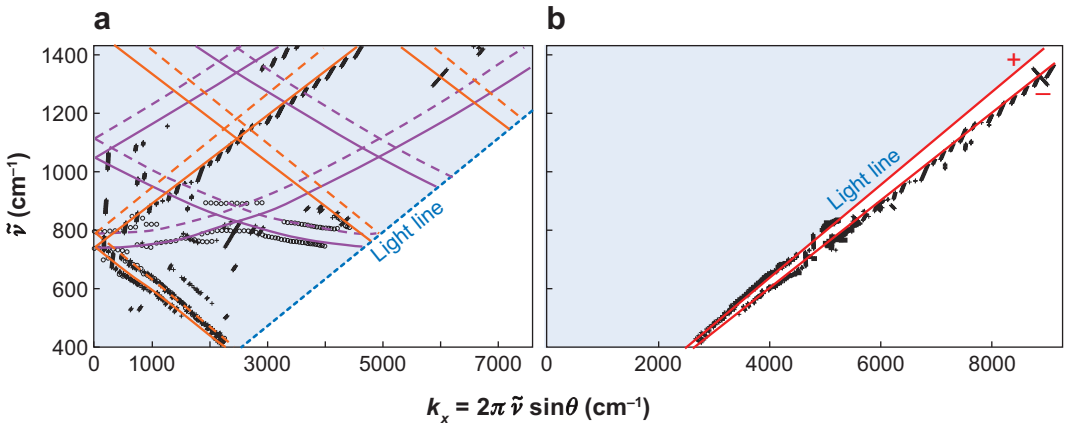

Figure 5

Dispersion measurements and curve simulations (*a*) of an Ni mesh active in the mid-infrared region (square holes on a square lattice, $L = 12.7$ μm, $a = 5.2$ μm, and $b = 3.0$ μm, similar to the mesh in **Figure 1** but with smaller holes) that were projected by momentum-matching equations to the region of the light line (*b*). One of the resulting surface plasmon (SP) dispersion curves (*red lines*) lies directly on the light line (the curve denoted with the *plus sign*), and the other is pushed to higher momentum by $n'_{eff} = 1.061$ (the curve denoted with the *minus sign*). These curves are the manifestation of front-back coupling of SPs through the holes of the array.

approximately one wavelength of the incident light. Pockrand (50) moved beyond zero-order expectations and gave second-order analytical expressions for smooth coupled interfaces. Lalanne et al. (54), who performed modal calculations on grids showing a definitive role for SPs, also mentioned the error of comparing the shifts to zero-order expectations. We conclude that the experimental shifts of the grid SP dispersion curves are consistent with the coupling of propagating SPs on the front and back surfaces through the holes of the mesh.

The above-mentioned infrared experiments produced stronger coupling than the Ebbesen group's experiments because the thickness of the mesh was less, only ~20% of the resonant wavelength. We use plus-sign and minus-sign subscripts to denote the symmetric and asymmetric states, respectively. These splittings have also been observed by S.-C. Lee and coworkers (55) for metal grids on silicon, were anticipated by Ulrich (4) in his early studies, and have also been seen by Pang et al. (56) for the (0,±1) SP mode. In addition, Teeters-Kennedy (57) acquired further evidence for extensive front-back coupling using enhanced infrared absorption experiments (29) on alkanethiol self-assembled monolayers applied to just one side of the mesh. She observed an identical infrared absorption spectrum regardless of whether the monolayer was placed facing the spectrometer source or away from it. The SPs must run equally on both sides of the mesh to get this result. Teeters-Kennedy et al. (10) determined SP dispersion curves using data obtained only at perpendicular incidence. They have quantified the additional curvature of the propagating SP dispersion curve (i.e., change in the effective refraction index with wavelength). We are not aware of

any analytical theory for a grid's geometrical effect on n'_{eff} [as Pockrand (50) has produced for smooth metal films in SP-ATR experiments], but it would certainly be a welcome addition, enabling a more accurate prediction of the position of grid transmission resonances. In general, if we allow for the splitting associated with front-back coupling through the holes, grids show quantitatively characteristic propagating SP curves.

Other evidence exists for the role of SPs. In their famous paper, Ebbesen and coworkers (1) established the importance of metal for propagating SP properties on grids by substituting germanium for silver, producing a great reduction in the transmission resonances. Gao et al. (58) have substituted Si for Au with similar results. This has also been accomplished by letting Cu-coated meshes oxidize extensively (59), as shown in the zero-order transmission spectra of **Figure 6**. It is certainly worth keeping in mind that not all the light transmitted by a single mesh is mediated by propagating SPs. Certainly photons falling directly on holes can be transmitted by direct mechanisms or LSPs associated with the structure of the hole. Transmission immediately after creation (before, red trace) includes both SP-mediated and direct mechanisms. After the Cu was extensively oxidized and its surface became nonmetallic

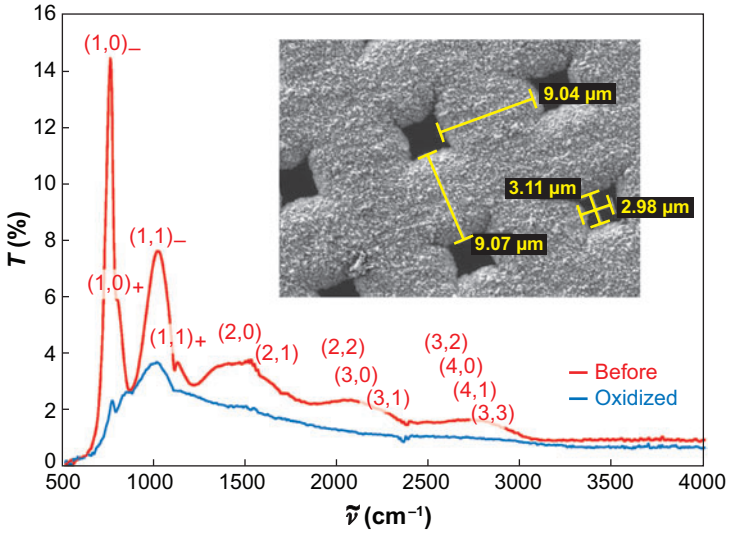

Figure 6

Zero-order transmission spectrum of an Ni mesh (similar to the one in **Figure 1**) that was electrochemically coated with Cu (as shown in the *inset*) closing the holes down to 3 μm. The red curve shows the transmission immediately after the mesh that was Cu-coated, and the blue curve shows the transmission after several months of oxidation, which diminished the metallic character of the surface. The blue curve represents non–surface plasmon (non-SP) mediated transmission (i.e., direct transmission mechanisms). If the blue curve is subtracted from the red curve, one obtains SP-resonant-dominated features. A metallic surface is clearly important for the SP resonances, but there are places in the spectrum at which direct mechanisms are also important in the transmission.

(a process that took several months), only the spectrum of the direct mechanisms was seen (blue trace) (59). The propagating SPs yield a much more structured spectrum than the direct transmission mechanism. The SP spectrum might be obtained by subtracting the blue trace from the red one. Although many investigators are particularly interested in the SP components of the transmitted light (and this component likely has the most potential in future applications), SPs do not compose the whole picture. Genet et al. (60) have attempted to unify disparate viewpoints by using a Fano (61) lineshape analysis with nonresonant and resonant contributions. The lineshapes are reasonably modeled, and the resonant contributions correlate with a role for SPs (60). More dramatically, the blue spectrum of direct mechanisms (**Figure 6**) can be greatly diminished by stacking two meshes, one on top of the other, so that there is always the metal of the second mesh behind the holes of the first (10). Incidentally, such double stacks have an infinite enhancement factor by the criteria of transmittance over fractional open area, which speaks to arguments against SP models made because enhancements on single meshes have not exceeded approximately seven (62). Along these lines, it is possible to see similar, but less intense, transmission resonances with grids of materials that are not good metals [such as Cr (63, 64) and W (62, 65)]. However, one does better in practice with good metals in which the eigenmodes are SPs (64).

Polarization properties (9, 10) are also telling with regard to the role of SPs. Whereas one-dimensional gratings only see *p*-polarized activity (**Figure 3*a***), bigrating resonances with $j > 0$ exhibit *s*-polarization activity (**Figure 3*b***). Williams & Coe carefully examined the initially flat, but ultimately quadratic, dispersion trend of the *s*-polarized $(0,\pm1)$ transmission resonance (11; see equation 4 therein) and found it to be rigorously predicted by the SP momentum-matching equations. Barnes et al. (9) have measured both the zero-order reflection and transmission of a grid to determine the zero-order absorption ($A = 1\text{-}R\text{-}T$) or the dissipative behavior of the mesh. They found that absorbance increases correlated with the transmission maxima and reflection minima, as expected for propagating SPs. Finally, Odom and coworkers (58, 66) have imaged SPs on grids in the near field and modeled them with finite-difference time-domain calculations, supporting a role for SPs.

THE EFFECT OF *L*

The most important parameter in designing a mesh for an application is *L* (see Equation 1), the hole-to-hole spacing or lattice parameter. This is the key factor for those interested in tuning SP resonances to overlap with atomic and molecular phenomena of interest at specific frequencies. **Figure 7** shows spectra of grids with resonances ranging from the far-infrared to the visible regions of the electromagnetic spectrum. Crudely, the primary transmission resonances occur at ~1.1 L with variations at the 10% level owing to the strength of the front-back coupling through the holes. More accurate predictions will require empirical modeling or a theoretical treatment of the strength of the front-back coupling and/or radiation damping. Note that the meshes with mid-infrared and visible activity have smaller fractional open

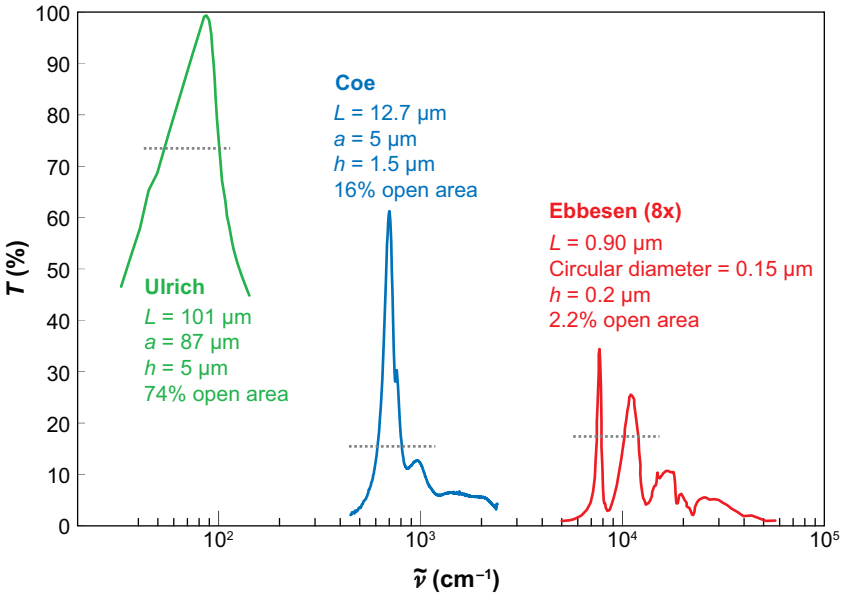

Figure 7

Zero-order transmission spectra of an Ulrich (4) grid with $L = 101$ μm (*green curve*), a Coe group grid with $L = 12.7$ μm (*blue curve*), and an Ebbesen group grid (1; see **Figure 1** therein) with $L = 0.90$ μm (*red*, intensity multiplied by a factor of 8), where L is the lattice spacing. A log scale on the abscissa illustrates the large range of frequencies that can be accessed by tuning L. The percentage of open area is plotted with a gray dotted line for each spectrum. Note also that the smaller percentage of open areas in the Coe and Ebbesen grids helps to reduce direct transmission mechanisms relative to the surface plasmon–mediated resonances.

areas that help to reduce the direct transmission mechanisms and enhance the SP features.

RESONANCE LINEWIDTHS

Relation to Propagation Lengths

The intrinsic linewidth of SPs on smooth air/metal interfaces is given by $2\,(2\pi\tilde{\nu}\mathrm{Im}\,(\varepsilon_{\mathbf{m}}\varepsilon_s/(\varepsilon_{\mathbf{m}}+\varepsilon_s)))$, where $\varepsilon_{\mathbf{m}}$ and ε_s are the complex dielectric permittivities of the metal and substrate, respectively (34). Ebbesen and colleagues' $(1,0)_{\mathrm{quartz}}$ resonance (1) on silver mesh, at 1.35 μm, has an intrinsic linewidth (full width at half-maximum) of 226 cm^{-1} [using $\varepsilon_{\mathbf{m}} = -67 + i6.6$ and $\varepsilon_s = 2.16$ (67)], which corresponds to the intrinsic $1/e$ propagation distance of 44 μm or ~49 holes. The observed full width at half-maximum was ~410 cm^{-1}, which is not that far from the intrinsic limit. If radiation damping is the loss mechanism (it could also be surface roughness, lack of lattice or hole uniformity, and so on), then SPs could conceivably be traveling across ~27 holes on resonance. The Coe group's $(1,0)_{-,\mathrm{air}}$ resonance

from **Figure 1** on Ni, at 701 cm^{-1}, has an intrinsic linewidth of 0.84 cm^{-1} [using $\varepsilon_m = -2331 + i1437$ and $\varepsilon_s = 1.00$ (67)] and an intrinsic propagation distance of 1.1 cm or 866 holes. The observed linewidth of 92 cm^{-1} is considerably larger, suggesting that SPs could be traveling approximately eight holes on this resonance. There seems to be more room for narrowing the resonances in the infrared region. The resonances with higher values of (i, j) get broader (see **Figure 6**), as was anticipated by Ulrich (4) because "the higher the frequency of a guided wave, the more of its SHs [space harmonics] fall into the radiative region." Studies in the near-infrared (68) and terahertz regions (69), as well as modeling by Genet et al. (60) and Muller et al. (70), also provide evidence for the importance of radiative damping. Note that whereas one SP-ATR prism device is inherently reflective, two stacked with a wavelength-scale spacing are coupled and become transmitters (i.e., radiation damping is so important that the device now transmits, and one can make measurements in transmission or reflection). A single piece of freestanding mesh is an optical analog of a wavelength-spaced stack of SP-ATR prisms, in that it shows two peaks owing to front-back coupling through the holes (of similar magnitude shifts to SP-ATR) and can be assayed in transmission (10).

In another approach to investigating SP propagation lengths, it is becoming clear that enhanced infrared absorption spectroscopy may be valuable. Using 12-μm-wide fields in an infrared microscope and noting that the strong 698-cm^{-1} vibration of polystyrene is well overlapped with the $(-1,0)_-$ resonance (if the mesh is tilted), we have been able to record the absorption spectrum of a 6-μm-wide clump of polystyrene microspheres at a distance as far away as 57 μm. The absorption signal versus distance has an exponential shape. Conversely, researchers have conducted enhanced infrared absorption experiments (29, 59, 71–74) using the extraordinary transmission effect on metallic microarrays. By comparing the grid absorptions (29) with those seen with reflection infrared absorption spectroscopy (75), investigators have deduced an average effective path length of ~8 μm (a bit smaller than L) for the portion of the spectrum far away from the (1,0) resonance. Vibrations on the (1,0) resonance can experience even greater enhancements (71) owing to longer propagation lengths and strong electric fields, among other effects.

Fitting Lineshapes

Williams et al. (2) performed a damped harmonic oscillator lineshape analysis on the (–1,0) resonance of freestanding Ni mesh at angles greater than $\theta = 10°$, where the resonance has dispersed away from other resonances and the splitting due to front-back coupling through the holes is the smallest. The mesh was tuned from 10°–75° dispersing the resonance from 646–398 cm^{-1} and producing significant narrowing. In fact the resonance Q value ($\tilde{\nu}/\Delta\tilde{\nu}_{FWHM}$) varied from 20 to 40 over this range. They also fit the reciprocal damped harmonic oscillator linewidths (i.e., lifetime reciprocals) to an exponential curve versus wavelength (λ) giving $6.6e^{\lambda/(5.8\mu m)}$. The exponential constant curiously matches the hole width.

In concluding this section, we note that Pockrand (50) has modeled SP-ATR experiments (smooth and thin metal films) using second-order theory including radiation

damping. All of our comparisons to mesh above are to the zero-order expectations, but we can gain understanding by looking at Pockrand's higher orders of approximation. He gives a complex term for radiation damping (50; see Equations 5 and 7 therein) in which the real part of this term gives the shift in momentum space owing to front-back coupling, and the imaginary part gives the increase in the width of resonances owing to radiative loss upon SP coupling to the second interface. Again, we send a plea to the theoretically inclined: An analogous treatment for these effects on grids would be useful.

THE EFFECT OF LATTICE, HOLE SHAPE, ORIENTATION, AND THICKNESS

Although most work on hole arrays is dominated by square lattices, hexagonal arrays possibly may be better. Thio et al. (63) made zero-order transmission measurements at perpendicular incidence on both hexagonal and square lattice arrays of Cr on quartz with similar fractional open areas (500-nm hole diameters, 1000-nm lattice constants, and 100-nm thickness). Although Cr is not a good metal for SPs and these experiments may be exciting Brewster-Zenneck modes (64) rather than SPs, the hexagonal array showed 40% transmission with 22.7% open area, whereas the square lattice array showed 28% transmission with 19.6% open area. For those interested in hexagonal lattices, these authors (63) also give the momentum-matching equations for a hexagonal lattice. Sun et al. (76) have investigated aperiodic concentric circular hole arrays (with sixfold rotational symmetry and inversion symmetry, but not translational symmetry) and found them to be six and two times better than comparable square and hexagonal lattices, respectively.

Koerkamp et al. (77) have shown with experiments and Fourier modal calculations that the extraordinary transmission of metal hole arrays is strongly influenced by the hole shape. Single holes have also been theoretically investigated by Garcia-Vidal et al. (78). Square holes are considerably better than round holes owing to the LSPs associated with the hole shapes, and rectangular shapes are better than circles or squares (79). Crosses, which in some sense contain two rectangular shapes, have also been shown to be good shapes for extraordinary transmission (3, 80). Ishihara & Ohashi (81) have performed finite-difference time-domain calculations suggesting that dimples within circular holes of square lattices can improve transmission by a factor of seven with their geometries. Kim & Moyer (82) made arrays with triangular holes and found them more transmitting than circles or squares. Diamond hole shapes (83) and H-shaped holes (84) have been investigated. Van Nieuwstadt et al. (85) have examined the effect of rectangular apertures on second-harmonic generation, which might have useful applications in nonlinear spectroscopy.

One can also obtain better transmission by filling the holes with dielectric material (86). As the polarization of the incident field selects the resonances excited on a lattice, Gordon et al. (87) have separated the effects of basis (hole shape) and lattice on transmission polarization by using elliptical holes that do not necessarily point in the same direction as the lattice. Several groups have examined the effect of hole width (88, 89), as well as film thickness (49). As the hole width was decreased, the

propagating SP dispersion trends flattened out (89). This was likely due to a transition from transmission dominated by propagating SP modes to LSPs (although this was not discussed by the authors). Murray et al. (33) have observed a transition from propagating to LSPs in studies of arrays of metal particles in which the particles grow and are merged into a mesh.

THE EFFECT OF COATING

The transmission resonances of metal grids are sensitive to the dielectric properties of nanoscale coatings, even when illuminated at perpendicular incidence (90). TiO_2 coatings of 60–105 nm thickness on Ni microarrays (similar to that of **Figure 1**) show shifts, attenuation, and broadening of the $(1,0)_-$ resonance from the uncoated positions. The shifts are in the range of 4–10 cm^{-1}, which is readily measured by standard benchtop Fourier transform infrared spectrometers. Hexadecane coatings (71) on Ni mesh on the scale of a few micrometers in thickness produce shifts of the $(1,0)_-$ resonance of $\sim$120 cm^{-1}. As the hexadecane film evaporates on exposure to the infrared beam of a Fourier transform infrared spectrometer, the resonance shifts back to its original, uncoated position at $\sim$750 cm^{-1}. Investigators used this effect to tune the SP resonance through a concerted rocking vibration of the molecule at 721 cm^{-1}. The interaction of the SP and vibrational excited state causes the vibrational absorption to become more intense, the lineshape to change, and the peak to shift by several wave numbers [on the order of changes seen with megavolt-per-centimeter fields in vibrational Stark spectroscopy (91)]. Whereas carbon coatings are known to be absorbing in the visible (34, 50), 300-nm-thick coatings act like windows in the infrared region. These observations encourage one to try nanoscale coatings comprising just about any material on the metallic meshes. Dintinger et al. (30) have used coatings of photochromic molecules on nanohole arrays to create fast, all-optical switching devices. They have also demonstrated strong coupling between SPs and J-aggregates in coatings (92).

THEORY OF EXTRAORDINARY TRANSMISSION ON GRIDS

Genet & Ebbesen's (8, and references therein) review gives a more exhaustive list of theoretical references regarding extraordinary transmission on grids. Popov et al. (13) showed that one-dimensional gratings have efficient channels for light transmission that do not exist for hole arrays, so the SP theory of one-dimensional slits (although interesting) may not be useful for explaining Ebbesen's extraordinary transmission effect on grids. In 1983, Glass et al. (19) studied the reflectivity resonances of SPs on sinusoidal bigratings with regard to the potential for surface-enhanced Raman spectroscopy. A great amount of theoretical interest accompanied Ebbesen et al.'s (1) 1998 paper that presented evidence of light coupling with SPs on the periodic metal grid. Several numerical simulations (93–96) appeared that illustrated the *E*-fields and supported the role of SPs. Martin-Moreno and colleagues presented a theory (and simpler model) that considered SPs on infinite grids coupling through an evanescent mode(s) of the hole. The authors only modeled the

data at perpendicular incidence and captured many (but not all) of the salient features of the experimental spectra. Muller et al. (70) did finite-difference time-domain simulations concentrating on the time-dependent SP coupling effects and radiation damping.

More recently, it has been noted that the enhanced transmissions of hole arrays can be obtained with calculations on perfect metal conductors (15, 97–101). Although perfect smooth metals do not support SPs, the introduction of geometric indentations can support bound surface waves with some similarities to the dispersion of SPs. Garcia-Vidal et al. (15) give a *p*-polarized dispersion curve that depends on the geometry and seems to level off at $\tilde{\nu}$ values of $\sim 1/L$ (47). Experimental dispersion spectra have some resonances with flat dispersions, like the $(0,\pm 1)$, but they are *s*-polarized. A careful look at dispersion behavior may be useful in evaluating the experimental evidence for Pendry surface waves. Clearly, it is important to have a metal grid to support propagating SPs, but the importance of the metal's imaginary components of dielectric permittivity is likely overshadowed on grids by the radiation damping associated with the arrival of SPs at holes. As we move from SPs on smooth metal surfaces to mesh arrays, there is clearly an increasingly important role for geometry. As we mentioned above (**Figure 6**), there are other contributions to mesh transmission besides SPs. Genet et al. (60) present a unifying view, whereby they used a Fano (61) analysis to fit experimental lineshapes considering resonant and nonresonant mechanisms. Sarrazin et al. (102) suggested something similar. It seems that the extraordinary transmission of hole arrays is more general than previously appreciated. Sarrazin & Vigneron (64) have confirmed that other kinds of electromagnetic modes besides SPs can participate in extraordinary transmission in hole arrays. They described Brewster-Zenneck modes, rather than SPs, to explain the extraordinary transmission with bad SP metals, such as Cr and W. Finally, there are alternative explanations (62, 103, 104) under consideration for the extraordinary transmission of metal hole arrays, so the role of SPs is not fully settled. It seems fair to say at this point that most investigators admit some role for SPs, and some a great role (54), although they might be admixed with various other forms of electromagnetic radiation.

APPLICATIONS

Enhanced spectroscopy is one of the most important applications of the extraordinary transmission effect. Fluorescence (28, 105), surface-enhanced Raman (21), visible absorption (30), and infrared absorption spectroscopy (2, 29, 59, 71–73) have all been enhanced using metal arrays of subwavelength holes. **Figure 8** shows the enhanced infrared absorption of alkanethiol self-assembled monolayers on Cu-coated Ni mesh. The absorptions are approximately a factor of 300-fold enhanced over reflection infrared absorption spectroscopy spectra. There is also evidence of strong coupling between molecules and the SP field in both the visible (92) and the infrared (71). Because light on mesh becomes two-dimensional when SPs are excited, there is great potential for enclosing and assaying spectroscopically the subwavelength spaces between two pieces of metal mesh. We created double stacks of mesh (10, 73, 74), and

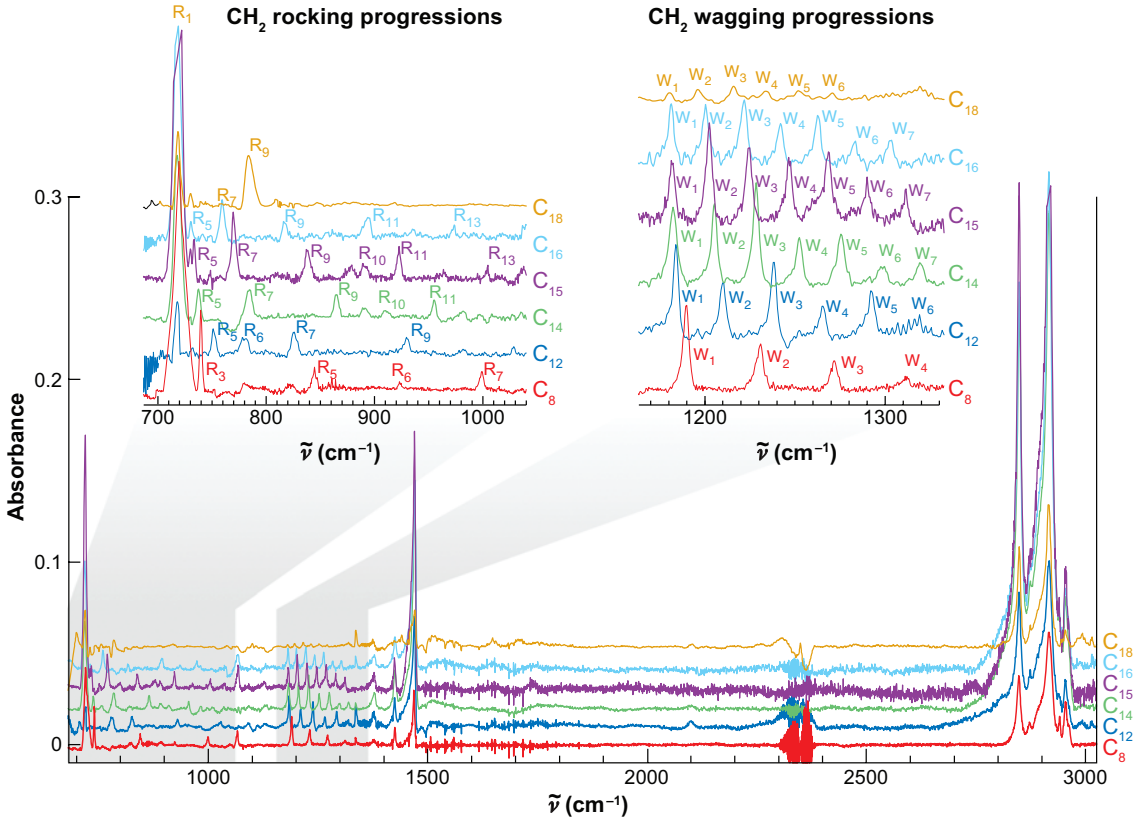

Figure 8

Enhanced infrared absorption spectra of alkanethiol self-assembled monolayers (SAMs) on Ni grids with Cu coatings (similar to those shown in the inset of **Figure 6** but with larger holes). Traces are shown for hydrocarbon chains from 8–18 carbon atoms. The absorptions in the CH-stretching region are ~300 larger than reflection infrared absorption spectra of the same species on smooth metal films. The CH_2 wagging and rocking progressions are only observed for all-*trans* hydrocarbon chains and have not been previously observed for alkanethiol SAMs. Both these regions have been expanded in the insets.

one had two pieces in registry such that there was always metal of the second mesh behind the holes of the first (10). The zero-order transmission spectra are shown in **Figure 9**. Even though the stack in **Figure 9*c*** has zero open area, it still transmits a working quantity of infrared radiation. By the single mesh criteria of transmittance divided by fractional open area, this is an infinite enhancement. Metal meshes with subwavelength holes have been used for ultrafast switching (30, 106), launching and decoupling SPs (107), collecting light from emitting diodes (108), biosensing (109), SP-mediated thermal emission (110–112), and contrast improvement in Moire fringes (113). SP photonic meshes show great promise.

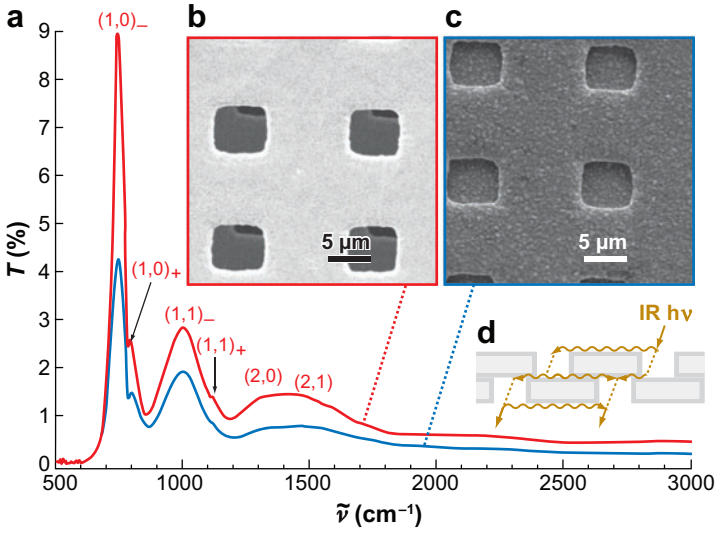

Figure 9

(*a*) Zero-order transmission spectra of stacks of Ni micromeshes as pictured with scanning electron microscope images in *b* and *c*. The stacks comprise two pieces, each similar to the mesh pictured in **Figure 1**. Both stacks are in registry, but the one in panel *c* has zero open area. It still transmits ~4% of the incident radiation. By the criteria of transmittance divided by fractional open area, this is an infinite enhancement. A cartoon of the surface plasmons (SPs) is given in panel *d*. The two-dimensional nature of SPs suggests that such stacks can be used to enclose nanoscale spaces between the meshes to be assayed with light of much larger wavelength.

CONCLUSION

SP photonic meshes represent a new opportunity to integrate SPs with experiments and devices—a new instrument that may broaden the range of SP applications. They offer a new set of tools for accomplishing experiments in small spaces, with high electric fields, and/or long path lengths for absorption.

DISCLOSURE STATEMENT

The authors are not aware of any biases that might be perceived as affecting the objectivity of this review.

ACKNOWLEDGMENT

We thank the National Science Foundation for supporting this work under grant number CHE-0413077 and the ACS PRF under grant numbers 38502-AC5 and 42452-AC5.

LITERATURE CITED

1. Ebbesen TW, Lezec HJ, Ghaemi HF, Thio T, Wolff PA. 1998. Extraordinary optical transmission through subwavelength hole arrays. *Nature* 391:667–69
2. Williams SM, Stafford AD, Rodriguez KR, Rogers TM, Coe JV. 2003. Accessing surface plasmons with Ni microarrays for enhanced IR absorption by monolayers. *J. Phys. Chem. B* 107:11871–79
3. Moller KD, Farmer KR, Ivanov DVP, Sternberg O, Stewart KP, Lalanne P. 1999. Thin and thick cross shaped metal grids. *Infrared Phys. Technol.* 40:475–85
4. Ulrich R. 1975. Modes of propagation on an open periodic waveguide for the far infrared. *Symp. Opt. Acoust. Microelectron., New York, April 16–18, 1974*, pp. 359–76. Brooklyn: Polytechn. Inst. New York
5. Ulrich R. 1967. Far-infrared properties of metallic mesh and its complementary structure. *Infrared Phys.* 7:37–55
6. Derrick GH, McPhedran RC, Maystre D, Neviere M. 1979. Crossed gratings: a theory and its applications. *Appl. Phys.* 18:39–52
7. McPhedran RC, Maystre D. 1977. On the theory and solar application of inductive grids. *Appl. Phys.* 14:1–20
8. Genet C, Ebbesen TW. 2007. Light in tiny holes. *Nature* 445:39–46
9. Barnes WL, Murray WA, Dintinger J, Devaux E, Ebbesen TW. 2004. Surface plasmon polaritons and their role in the enhanced transmission of light through periodic arrays of subwavelength holes in a metal film. *Phys. Rev. Lett.* 92:107401
10. Teeters-Kennedy SM, Williams SM, Rodriguez KR, Cilwa K, Meleason D, et al. 2007. Extraordinary infrared transmission of a stack of two metal micromeshes. *J. Phys. Chem. C* 111:124–30
11. Williams SM, Coe JV. 2006. Dispersion study of the infrared transmission resonances of freestanding Ni microarrays. *Plasmonics* 1:87–93
12. Qu D, Grischkowsky D. 2004. Observation of a new type of THz resonance of surface plasmons propagating on metal-film hole arrays. *Phys. Rev. Lett.* 93:196804
13. Popov E, Neviere M, Enoch S, Reinisch R. 2000. Theory of light transmission through subwavelength periodic hole arrays. *Phys. Rev. B Condens. Matter Mater. Phys.* 62:16100–8
14. Ghaemi HF, Thio T, Grupp DE, Ebbesen TW, Lezec HJ. 1998. Surface plasmons enhance optical transmission through subwavelength holes. *Phys. Rev. B Condens. Matter Mater. Phys.* 58:6779–82
15. Garcia-Vidal FJ, Martin-Moreno L, Pendry JB. 2005. Surfaces with holes in them: new plasmonic metamaterials. *J. Opt. A* 7:S97–101
16. Willets KA, Van Duyne RP. 2007. Localized surface plasmon resonance spectroscopy and sensing. *Annu. Rev. Phys. Chem.* 58:267–97
17. Haes AJ, Van Duyne RP. 2004. A unified view of propagating and localized surface plasmon resonance biosensors. *Anal. Bioanal. Chem.* 379:920–30
18. Andersen PC, Rowlen KL. 2002. Brilliant optical properties of nanometric noble metal spheres, rods, and aperture arrays. *Appl. Spectrosc.* 56:A124–35
19. Glass NE, Maradudin AA, Celli V. 1983. Diffraction of light by a bigrating: surface polariton resonances and electric-field enhancements. *Phys. Rev. B Condens. Matter* 27:5150–53

20. Kneipp K, Kneipp H, Manoharan R, Hanlon EB, Itzkan I, et al. 1998. Extremely large enhancement factors in surface-enhanced Raman scattering for molecules on colloidal gold clusters. *Appl. Spectrosc.* 52:1493–97
21. Brolo AG, Arctander E, Gordon R, Leathem B, Kavanagh K. 2004. Nanohole-enhanced Raman scattering. *Nano Lett.* 4:2015–18
22. Fang N, Lee H, Sun C, Zhang X. 2005. Sub-diffraction-limited optical imaging with a silver superlens. *Science* 308:534–37
23. Yin L, Vlasko-Vlasov VK, Rydh A, Pearson J, Welp U, et al. 2004. Surface plasmons at single nanoholes in Au films. *Appl. Phys. Lett.* 85:467–69
24. Fang N, Zhang X. 2003. Imaging properties of a metamaterial superlens. *Appl. Phys. Lett.* 82:161–63
25. Fang N, Liu Z, Yen T-J, Zhang X. 2003. Regenerating evanescent waves from a silver superlens. *Opt. Expr.* 11:682–87
26. Ozbay E. 2006. Plasmonics: merging photonics and electronics at nanoscale dimensions. *Science* 311:189–93
27. Lakowicz JR. 2004. Radiative decay engineering 3. Surface plasmon-coupled directional emission. *Anal. Biochem.* 324:153–69
28. Brolo AG, Kwok SC, Moffitt MG, Gordon R, Riordon J, Kavanagh KL. 2005. Enhanced fluorescence from arrays of nanoholes in a gold film. *J. Am. Chem. Soc.* 127:14936–41
29. Rodriguez KR, Shah S, Williams SM, Teeters-Kennedy S, Coe JV. 2004. Enhanced infrared absorption spectra of self-assembled alkanethiol monolayers using the extraordinary infrared transmission of metallic arrays of subwavelength apertures. *J. Chem. Phys.* 121:8671–75
30. Dintinger J, Klein S, Ebbesen TW. 2006. Molecule-surface plasmon interactions in hole arrays: enhanced absorption, refractive index changes, and all-optical switching. *Adv. Mater.* 18:1267–70
31. Schouten HF, Kuzmin N, Dubois G, Visser TD, Gbur G, et al. 2005. Plasmon-assisted two-slit transmission: Young's experiment revisited. *Phys. Rev. Lett.* 94:053901
32. Hao E, Schatz GC. 2004. Electromagnetic fields around silver nanoparticles and dimers. *J. Chem. Phys.* 120:357–66
33. Murray WA, Astilean S, Barnes WL. 2004. Transition from localized surface plasmon resonance to extended surface plasmon-polariton as metallic nanoparticles merge to form a periodic hole array. *Phys. Rev. B Condens. Matter Mater. Phys.* 69:165407
34. Raether H. 1988. *Surface Plasmons on Smooth and Rough Surfaces and on Gratings*. Berlin: Springer-Verlag. 136 pp.
35. Welford K. 1991. Surface plasmon-polaritons and their uses. *Opt. Quantum Electron.* 23:1–27
36. Otto A. 1968. Excitation of nonradiative surface plasma waves in silver by the method of frustrated total reflection. *Z. Phys.* 216:398–410
37. Kretschmann E, Raether H. 1968. Radiative decay of nonradiative surface plasmons excited by light. *Z. Nat. A* 23:2135–36

38. Liu W-C, Tsai DP. 2002. Optical tunneling effect of surface plasmon polaritons and localized surface plasmon resonance. *Phys. Rev. B Condens. Matter Mater. Phys.* 65:155423
39. Sarychev AK, Podolskiy VA, Dykhne AM, Shalaev VM. 2002. Resonance transmittance through a metal film with subwavelength holes. *IEEE J. Quantum Electron.* 38:956–63
40. Wood RW. 1902. On a remarkable case of uneven distribution of light in a diffraction grating spectrum. *Philos. Mag.* 4:396–402
41. Rayleigh L. 1907. Note on the remarkable case of diffraction spectra described by Prof. Wood. *Philos. Mag.* 14:60–65
42. Strong J. 1936. Effect of evaporated films on energy distribution in grating spectra. *Phys. Rev.* 49:291–96
43. Hagglund J, Sellberg F. 1966. Reflection, absorption, and emission of light by opaque optical gratings. *J. Opt. Soc. Am.* 56:1031–40
44. Hessel A, Oliner AA. 1965. A new theory of Wood's anomalies on optical gratings. *Appl. Opt.* 4:1275–97
45. Ritchie RH, Arakawa ET, Cowan JJ, Hamm RN. 1968. Surface-plasmon resonance effect in grating diffraction. *Phys. Rev. Lett.* 21:1530–33
46. Schroter U, Heitmann D. 1998. Surface-plasmon-enhanced transmission through metallic gratings. *Phys. Rev. B Condens. Matter Mater. Phys.* 58:15419–21
47. Williams SM. 2006. *Characteristics and applications of the infrared enhanced transmission of metallic subwavelength arrays*. PhD thesis. Ohio State Univ., Columbus. 405 pp.
48. Pullman A, Ebbesen T, Rholam M. 1979. Cation binding to biomolecules. VI. SCF ab initio (pseudopotential) computations on the interaction of zinc (2+) with the purine and pyrimidine bases of the nucleic acids. *Theor. Chim. Acta* 51:247–54
49. Degiron A, Lezec HJ, Barnes WL, Ebbesen TW. 2002. Effects of hole depth on enhanced light transmission through subwavelength hole arrays. *Appl. Phys. Lett.* 81:4327–29
50. Pockrand I. 1978. Surface plasma oscillations at silver surfaces with thin transparent and absorbing coatings. *Surf. Sci.* 72:577–88
51. Yang F, Bradberry GW, Sambles JR. 1990. Coupled surface plasmons at 3.391 mm. *J. Mod. Opt.* 37:993–1003
52. Economou EN. 1969. Surface plasmons in thin films. *Phys. Rev.* 182:539–54
53. Fuzi Y, Bradberry GW, Sambles JR. 1989. Infrared surface plasmon-polaritons on nickel, palladium, and platinum. *J. Mod. Opt.* 36:1405–10
54. Lalanne P, Rodier JC, Hugonin JP. 2005. Surface plasmons of metallic surfaces perforated by nanohole arrays. *J. Opt. A* 7:422–26
55. Tsai M-W, Chuang T-H, Chang H-Y, Lee S-C. 2006. Bragg scattering of surface plasmon polaritons on extraordinary transmission through silver periodic perforated hole arrays. *Appl. Phys. Lett.* 88:213112
56. Pang L, Tetz KA, Fainman Y. 2007. Observation of the splitting of degenerate surface plasmon polariton modes in a two-dimensional metallic nanohole array. *Appl. Phys. Lett.* 90:111103

57. Teeters-Kennedy S. 2007. *Infrared surface plasmons in double stacked nickel microarrays: lipid bilayer systems*. PhD thesis. Ohio State Univ., Columbus
58. Gao HW, Henzie J, Odom TW. 2006. Direct evidence for surface plasmon-mediated enhanced light transmission through metallic nanohole arrays. *Nano Lett.* 6:2104–8
59. Williams SM, Rodriguez KR, Teeters-Kennedy S, Stafford AD, Bishop SR, et al. 2004. Use of the extraordinary infrared transmission of metallic subwavelength arrays to study the catalyzed reaction of methanol to formaldehyde on copper oxide. *J. Phys. Chem. B* 108:11833–37
60. Genet C, van Exter MP, Woerdman JP. 2003. Fano-type interpretation of red shifts and red tails in hole array transmission spectra. *Opt. Commun.* 225:331–36
61. Fano U. 1941. The theory of anomalous diffraction grating and of quasi-stationary waves on metallic surfaces (Sommerfield's waves). *J. Opt. Soc. Am.* 31:213–22
62. Lezec HJ, Thio T. 2004. Diffracted evanescent wave model for enhanced and suppressed optical transmission through subwavelength hole arrays. *Opt. Exp.* 12:3629–51
63. Thio T, Ghaemi HF, Lezec HJ, Wolff PA, Ebbesen TW. 1999. Surface-plasmon-enhanced transmission through hole arrays in Cr films. *J. Opt. Soc. Am. B* 16:1743–48
64. Sarrazin M, Vigneron J-P. 2005. Light transmission assisted by Brewster-Zenneck modes in chromium films carrying a subwavelength hole array. *Phys. Rev. B* 71:075404
65. Sarrazin M, Vigneron J-P. 2003. Optical properties of tungsten thin films perforated with a bidimensional array of subwavelength holes. *Phys. Rev. E* 68:016603
66. Kwak E-S, Henzie J, Chang S-H, Gray SK, Schatz GC, Odom TW. 2005. Surface plasmon standing waves in large-area subwavelength hole arrays. *Nano Lett.* 5:1963–67
67. Rakic AD, Djurisic AB, Elazar JM, Majewski ML. 1998. Optical properties of metallic films for vertical-cavity optoelectronic devices. *Appl. Opt.* 37:5271–83
68. Kim DS, Hong SC, Malyarchuk V, Yoon YC, Ahn YH, et al. 2003. Microscopic origin of surface-plasmon radiation in plasmonic band-gap nanostructures. *Phys. Rev. Lett.* 91:143901
69. Naweed A, Baumann F, Bailey WA Jr, Karakashian AS, Goodhue WD. 2003. Evidence for radiative damping in surface-plasmon-mediated light transmission through perforated conducting films. *J. Opt. Soc. Am. B* 20:2534–38
70. Muller R, Malyarchuk V, Lienau C. 2003. Three-dimensional theory of light-induced near-field dynamics in a metal film with a periodic array of nanoholes. *Phys. Rev. B* 68:205415
71. Rodriguez KR, Tian H, Heer JM, Teeters-Kennedy SM, Cilwa K, Coe JV. 2007. Interaction of an infrared surface plasmon with a molecular vibration. *J. Chem. Phys.* 126:151101
72. Teeters-Kennedy SM, Rodriguez KR, Rogers TM, Zomchek KA, Williams SM, et al. 2006. Controlling the passage of light through metal microchannels by nanocoatings of phospholipids. *J. Phys. Chem. B* 110:21719–27

73. Coe JV, Williams SM, Rodriguez KR, Teeters-Kennedy S, Sudnitsyn A, Hrovat F. 2006. Extraordinary IR transmission with metallic arrays of subwavelength holes. *Anal. Chem.* 78:1385–90
74. Williams SM, Rodriguez KR, Teeters-Kennedy S, Shah S, Rogers TM, et al. 2004. Scaffolding for nanotechnology: extraordinary infrared transmission of metal microarrays for stacked sensors and surface spectroscopy. *Nanotechnology* 15:S495–507
75. Laibinis PE, Whitesides GM, Allara DL, Tao Y-T, Parikh AN, Nuzzo RG. 1991. Comparison of the structures and wetting properties of self-assembled monolayers of *n*-alkanethiols on the coinage metal surfaces, Cu, Ag, Au. *J. Am. Chem. Soc.* 113:7152–67
76. Sun M, Tian J, Han SZ, Li ZY, Cheng BY, et al. 2006. Effect of the subwavelength hole symmetry on the enhanced optical transmission through metallic films. *J. Appl. Phys.* 100:024320
77. Koerkamp KJK, Enoch S, Segerink FB, van Hulst NF, Kuipers L. 2004. Strong influence of hole shape on extraordinary transmission through periodic arrays of subwavelength holes. *Phys. Rev. Lett.* 92:183901
78. Garcia-Vidal FJ, Moreno E, Porto JA, Martin-Moreno L. 2005. Transmission of light through a single rectangular hole. *Phys. Rev. Lett.* 95:103901
79. van der Molen KL, Klein Koerkamp KJ, Enoch S, Segerink FB, van Hulst NF, Kuipers L. 2005. Role of shape and localized resonances in extraordinary transmission through periodic arrays of subwavelength holes: experiment and theory. *Phys. Rev. B Condens. Matter Mater. Phys.* 72:045421
80. Moller KD, Sternberg O, Grebel H, Lalanne P. 2002. Thick inductive cross shaped metal meshes. *J. Appl. Phys.* 91:9461–65
81. Ishihara K, Ohashi K. 2005. Strong influence of surface structures on enhanced transmission through subwavelength hole arrays. *Jpn. J. Appl. Phys.* 44:L973–75
82. Kim JH, Moyer PJ. 2006. Transmission characteristics of metallic equilateral triangular nanohole arrays. *Appl. Phys. Lett.* 89:121106
83. Sun M, Liu RJ, Li ZY, Cheng BY, Zhang DZ, et al. 2006. The influence of hole shape on enhancing transmission through subwavelength hole arrays. *Chin. Phys.* 15:1591–94
84. Sun M, Liu R-J, Li Z-Y, Cheng B-Y, Zhang D-Z, et al. 2007. Enhanced near-infrared transmission through periodic H-shaped arrays. *Phys. Lett. A* 365:510–13
85. van Nieuwstadt JAH, Sandtke M, Harmsen RH, Segerink FB, Prangsma JC, et al. 2006. Strong modification of the nonlinear optical response of metallic subwavelength hole arrays. *Phys. Rev. Lett.* 97:146102
86. Chen YG, Wang YH, Zhang Y, Lu ST. 2007. Numerical investigation of the transmission enhancement through subwavelength hole array. *Opt. Commun.* 274:236–40
87. Gordon R, Hughes M, Leathem B, Kavanagh KL, Brolo AG. 2005. Basis and lattice polarization mechanisms for light transmission through nanohole arrays in a metal film. *Nano Lett.* 5:1243–46

88. van der Molen KL, Segerink FB, van Hulst NF, Kuipers L. 2004. Influence of hole size on the extraordinary transmission through subwavelength hole arrays. *Appl. Phys. Lett.* 85:4316–18
89. Williams SM, Stafford AD, Rogers TM, Bishop SR, Coe JV. 2004. Extraordinary infrared transmission of Cu-coated arrays with subwavelength apertures: hole size and the transition from surface plasmon to waveguide transmission. *Appl. Phys. Lett.* 85:1472–74
90. Rodriguez KR, Tian H, Heer JM, Coe JV. 2007. Extraordinary infrared transmission resonances of metal microarrays for sensing nanocoating thickness. *J. Phys. Chem.* 111:12106–11
91. Brewster SH, Franzen S. 2003. A quantitative theory and computational approach for the vibrational Stark effect. *J. Chem. Phys.* 119:851–58
92. Dintinger J, Klein S, Bustos F, Barnes WL, Ebbesen TW. 2005. Strong coupling between surface plasmon-polaritons and organic molecules in subwavelength hole arrays. *Phys. Rev. B Condens. Matter Mater. Phys.* 71:035424
93. Salomon L, Grillot F, Zayats AV, de Fornel F. 2001. Near-field distribution of optical transmission of periodic subwavelength holes in a metal film. *Phys. Rev. Lett.* 86:1110–13
94. Krishnan A, Thio T, Kim TJ, Lezec HJ, Ebbesen TW, et al. 2001. Evanescently coupled resonance in surface plasmon enhanced transmission. *Opt. Commun.* 200:1–7
95. Wannemacher R. 2001. Plasmon-supported transmission of light through nanometric holes in metallic thin films. *Opt. Commun.* 195:107–18
96. Minhas BK, Fan W, Agi K, Brueck SRJ, Malloy KJ. 2002. Metallic inductive and capacitive grids: theory and experiment. *J. Opt. Soc. Am. A* 19:1352–59
97. Bravo-Abad J, Garcia-Vidal FJ, Martin-Moreno L. 2004. Resonant transmission of light through finite chains of subwavelength holes in a metallic film. *Phys. Rev. Lett.* 93:227401
98. Selcuk S, Woo K, Tanner DB, Hebard AF, Borisov AG, Shabanov SV. 2006. Trapped electromagnetic modes and scaling in the transmittance of perforated metal films. *Phys. Rev. Lett.* 97:067403
99. Lomakin V, Michielssen E. 2005. Enhanced transmission through metallic plates perforated by arrays of subwavelength holes and sandwiched between dielectric slabs. *Phys. Rev. B* 71:235117
100. Tanaka T, Akazawa M, Sano E, Tanaka M, Miyamaru F, Hangyo M. 2006. Transmission characteristics through two-dimensional periodic hole arrays perforated in perfect conductors. *Jpn. J. Appl. Phys.* 45:4058–63
101. Bravo-Abad J, Martin-Moreno L, Garcia-Vidal FJ. 2006. Resonant transmission of light through subwavelength holes in thick metal films. *IEEE J. Sel. Top. Quantum Electron.* 12:1221–27
102. Sarrazin M, Vigneron J-P, Vigoureux J-M. 2003. Role of Wood anomalies in optical properties of thin metallic films with a bidimensional array of subwavelength holes. *Phys. Rev. B Condens. Matter Mater. Phys.* 67:085415
103. Treacy MMJ. 2002. Dynamical diffraction explanation of the anomalous transmission of light through metallic gratings. *Phys. Rev. B* 66:195105

104. Jia W, Liu X. 2005. Origin of superenhanced light transmission through two-dimensional subwavelength rectangular hole arrys. *Eur. Phys. J. B* 46:343–47
105. Rigneault H, Capoulade J, Dintinger J, Wenger J, Bonod N, et al. 2005. Enhancement of single-molecule fluorescence detection in subwavelength apertures. *Phys. Rev. Lett.* 95:117401
106. Dintinger J, Robel I, Kamat PV, Genet C, Ebbesen TW. 2006. Terahertz all-optical molecule-plasmon modulation. *Adv. Mater.* 18:1645–48
107. Devaux E, Ebbesen TW, Weeber J-C, Dereux A. 2003. Launching and decoupling surface plasmons via micrograting. *Appl. Phys. Lett.* 83:4936–38
108. Liu C, Kamaev V, Vardeny ZV. 2005. Efficiency enhancement of an organic light-emitting diode with a cathode forming two-dimensional periodic hole array. *Appl. Phys. Lett.* 86:143501
109. Lesuffleur A, Im H, Lindquist NC, Oh S-H. 2007. Periodic nanohole arrays with shape-enhanced plasmon resonance as real-time biosensors. *Appl. Phys. Lett.* 90:243110
110. Kreiter M, Oster J, Sambles R, Herminghaus S, Mittler-Neher S, Knoll W. 1999. Thermally induced emission of light from a metallic diffraction grating, mediated by surface plasmons. *Opt. Commun.* 168:117–22
111. Biswas R, Ding CG, Puscasu I, Pralle M, McNeal M, et al. 2006. Theory of subwavelength hole arrays coupled with photonic crystals for extraordinary thermal emission. *Phys. Rev. B Condens. Matter Mater. Phys.* 74:045107
112. Tsai M-W, Chuang T-H, Meng C-Y, Chang Y-T, Lee S-C. 2006. High performance midinfrared narrow-band plasmonic thermal emitter. *Appl. Phys. Lett.* 89:173116
113. Liu Z, Durant S, Lee H, Xiong Y, Pikus Y, et al. 2007. Near-field Moire effect mediated by surface plasmon polariton excitation. *Opt. Lett.* 32:629–31

Annual Review of
Physical Chemistry

Volume 59, 2008

Contents

Indexes

Errata

An online log of corrections to *Annual Review of Physical Chemistry* articles may be found at http://physchem.annualreviews.org/errata.shtml